Stem Cell Reports
Article

OPEN ACCESS

DNA Methyltransferases Modulate Hepatogenic Lineage Plasticity of Mesenchymal Stromal Cells

Chien-Wei Lee,[1,14] Wei-Chih Huang,[3] Hsien-Da Huang,[3,4,5,6] Yi-Hsiang Huang,[7] Jennifer H. Ho,[8] Muh-Hwa Yang,[9,10,11,12,13] Vincent W. Yang,[17] and Oscar K. Lee[2,14,15,16,*]

[1]Program in Molecular Medicine, National Yang-Ming University and Academia Sinica, Taipei 11221, Taiwan
[2]Taipei City Hospital, Taipei 10341, Taiwan
[3]Institute of Bioinformatics and Systems Biology
[4]Department of Biological Science and Technology
[5]Center for Bioinformatics Research
National Chiao Tung University, HsinChu 30010, Taiwan
[6]Department of Biomedical Science and Environmental Biology, Kaohsiung Medical University, Kaohsiung 80708, Taiwan
[7]Division of Gastroenterology, Department of Medicine, Taipei Veterans General Hospital, Taipei 11221, Taiwan
[8]Center for Stem Cell Research, Taipei Medical University-Wan Fang Hospital, Taipei 11031, Taiwan
[9]Institute of Biotechnology in Medicine
[10]Genome Research Center
[11]Immunity and Inflammation Research Center
National Yang-Ming University, Taipei 11221, Taiwan
[12]Division of Hematology and Oncology, Department of Medicine, Taipei Veterans General Hospital, Taipei 11217, Taiwan
[13]Genomics Research Center, Academia Sinica, Taipei 11529, Taiwan
[14]Institute of Clinical Medicine, National Yang-Ming University
[15]Stem Cell Research Center, National Yang-Ming University
[16]Department of Medical Research, Taipei Veterans General Hospital
Taipei 11221, Taiwan
[17]Department of Medicine, Stony Brook University, Stony Brook, NY 11794, USA
*Correspondence: dav47@tpech.gov.tw
http://dx.doi.org/10.1016/j.stemcr.2017.05.008

SUMMARY

The irreversibility of developmental processes in mammalian cells has been challenged by rising evidence that de-differentiation of hepatocytes occurs in adult liver. However, whether reversibility exists in mesenchymal stromal cell (MSC)-derived hepatocytes (dHeps) remains elusive. In this study, we find that hepatogenic differentiation (HD) of MSCs is a reversible process and is modulated by DNA methyltransferases (DNMTs). DNMTs are regulated by transforming growth factor β1 (TGFβ1), which in turn controls hepatogenic differentiation and de-differentiation. In addition, a stepwise reduction in TGFβ1 concentrations in culture media increases DNMT1 and decreases DNMT3 in primary hepatocytes (Heps) and confers Heps with multi-differentiation potentials similarly to MSCs. Hepatic lineage reversibility of MSCs and lineage conversion of Heps are regulated by DNMTs in response to TGFβ1. This previously unrecognized TGFβ1-DNMTs-MSC-HD axis may further increase the understanding the normal and pathological processes in the liver, as well as functions of MSCs after transplantation to treat liver diseases.

INTRODUCTION

Hepatocytes possess de-differentiation and re-differentiation potential to achieve liver regeneration (Tarlow et al., 2014). Such findings have challenged the long-standing belief that differentiation is an irreversible process in mammals (Jopling et al., 2011; Metcalf, 2007). However, to date detailed mechanisms of how somatic cells undergo de-differentiation and subsequent re-differentiation remain undefined, and whether lineage reversibility exists in adult stem cells remains controversial (Zhau et al., 2011).

One useful model for studying lineage reversibility is the multi-potent mesenchymal stromal cells (MSCs) (Makino et al., 1999; Pittenger et al., 1999; Wislet-Gendebien et al., 2005), which can differentiate into hepatocyte-like cells (dHeps) (Jiang et al., 2014; Kuo et al., 2008; Lee et al., 2004) that possess therapeutic potentials for liver diseases. Currently, whether and how differentiated hepatic progenies from MSCs can be de-differentiated is unknown. Studies do show, however, DNA methylation plays an important role in controlling MSC differentiation (Tsai et al., 2012). DNA methyltransferases (DNMTs) control gene transcription and cellular phenotypic changes during liver organogenesis (Snykers et al., 2009). It has been reported that inhibition of DNMTs increases liver-specific gene expression to maintain a hepatic fate; a concomitant decrease of DNMT1 and increase of DNMT3 expression is associated with hepatic maturation in mouse hepatoblasts (Gailhouste et al., 2013). DNMT1 is the key to methylation maintenance, while DNMT3 is responsible for the initiation of de novo methylation (Li, 2002). However, the function roles of each DNMT in hepatic lineage commitment of MSCs are unknown. The purpose of this study is to investigate the hepatic lineage reversibility in MSCs as well as the

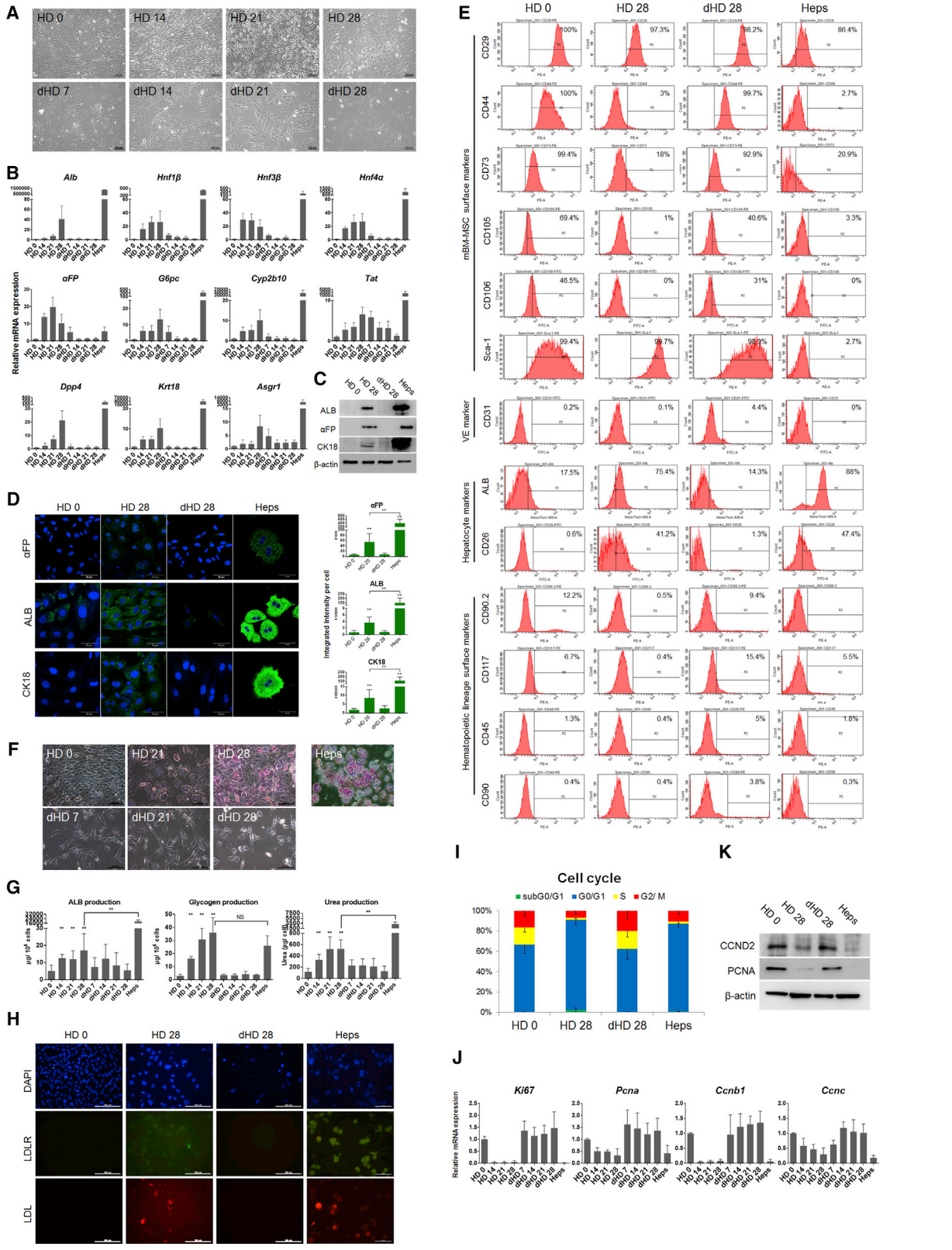

(legend on next page)

underlying molecular mechanisms. We hypothesize that alteration of culture conditions may achieve hepatic lineage reversibility between MSCs and their differentiated hepatic progenies.

RESULTS

Mouse MSC-Derived Differentiated Hepatocyte-like Cells Possess De-differentiation Potential

Mouse MSCs were induced into dHeps via our previously reported two-step protocol (Jiang et al., 2014; Kuo et al., 2008; Lee et al., 2004). During 4 weeks of hepatogenic differentiation (HD), the bipolar fibroblast-like morphology of the MSCs changed into cobblestone-like shapes from day 14 and then progressively changed into hexagonal shapes, a typical epithelial morphology at day 28 (Figure 1A). Expression of hepatocyte-specific genes was significantly upregulated after differentiation induction in a time-dependent manner (Figures 1B–1D). dHeps possessed hepatocyte surface markers similar to those of mouse Heps (Figure 1E).

The in vitro functional characteristics were further investigated by periodic acid-Schiff (PAS) staining (Figure 1F), measurements of glycogen, albumin, and urea production (Figure 1G), as well as low-density lipoprotein (LDL) uptake assays (Figure 1H). All the hepatic function markers significantly and progressively increased during differentiation. In general, although slightly lower, dHeps expressed function markers similar to those of Heps (Figures 1B–1H). Expression levels of hepatic-specific genes of dHeps are close to those of embryonic day 12.5 (E12.5) fetal livers and FL83B cells, and differ relatively from those of Heps (Figure S2). Compared with Heps, dHeps also expressed higher levels of Sca-1 (Figure 1E), Dlk1, and Cd24a (Figure S2), which are hepatic progenitor markers (Miyajima et al., 2014; Petersen et al., 2003; Qiu et al., 2011). These findings indicated that dHeps are similar to hepatic progenitors. Although dHeps are not identical to terminally differentiated mature Heps, they are committed hepatic cells.

After 28 days of HD, we de-differentiated dHeps by replacing differentiation medium with mouse MSC-maintenance medium for 28 days. Following hepatogenic de-differentiation (dHD), cellular morphology reverted back to fibroblast-like shapes (Figure 1A). Furthermore, liver-specific gene expression, surface marker presentation, and hepatic functions all switched back to the original levels observed in original MSCs (Figures 1B–1H).

We next examined cell-cycle profiles during HD and dHD. After differentiation for 28 days, the cells arrested at the G_0/G_1 phase but re-entered the cell cycle after de-differentiation for 28 days (Figure 1I). The reversibility of the cell cycle was accompanied by changes in expression of genes encoding cell-cycle checkpoint regulators as well as proliferation markers *Ki67* and *Pcna* (Figures 1J and 1K). The results indicated that hepatic lineage reversibility in MSCs was accompanied by cell-cycle exit and re-entry.

To explore the transcriptomic and proteomic changes during HD and dHD, we performed microarray analysis and high-density antibody arrays on MSCs (HD 0), dHeps (HD 28), and de-differentiated cells from dHeps (ddHeps, dHD 28). Hierarchical clustering (Figures 2A and 2B) showed that ddHeps clustered closely together with MSCs and were separated from dHeps and Heps. The profiles of genes involved in fibroblast markers, MSC markers (Figure 2C), lipid, glycolysis, cholesterol, and drug metabolism (Figure 2D) were very similar between dHeps and Heps, whereas ddHeps and MSCs displayed similar gene profiles. Collectively, these results indicated that the ddHep transcriptome and proteome had indeed reverted back to the MSC state.

Using the KEGG database, gene ontology was analyzed to understand the functional significance of differential gene expression during HD and dHD. Pathways involved in

Figure 1. Hepatogenic Differentiation and De-differentiation of Mouse Mesenchymal Stromal Cells

(A) Representative morphological changes in MSCs during hepatogenic differentiation (HD) and hepatogenic de-differentiation (dHD). Scale bar, 100 μm.

(B–D) Results of (B) qRT-PCR (n = 4 independent experiments), (C) a representative immunoblot, and (D) immunocytochemical staining for hepatogenic-specific gene expression. β-Actin was used as an internal control. Scale bar, 50 μm.

(E) Flow-cytometry analysis for surface phenotypic characterization.

(F) PAS (periodic acid-Schiff) staining for glycogen storage.

(G and H) Hepatic functions were measured via (G) albumin production (n = 7 independent experiments), glycogen storage (n = 4 independent experiments), urea production (n = 3 independent experiments), and (H) LDL-uptake assays. LDLR, LDL receptor.

(I) Results of flow-cytometry analysis showing the relative percentage of cells in various cell-cycle phases (n = 5 independent experiments).

(J and K) Results of (J) qRT-PCR (n = 4 independent experiments) and (K) a representative immunoblot for cell-cycle-related genes. "HD 0" refers to MSCs; "HD 28" refers to MSC-derived dHeps (hepatocyte-like cells) after 28 days of HD; "dHD 28" refers to dHep-derived ddHeps (de-differentiated cells) after 28 days of dHD; "Heps" refers to mouse primary hepatocytes.

All quantitative data are presented as means ± SD. Statistical analyses were performed using Student's paired t test, with significance set at $^{**}p < 0.001$. NS, not significant. See also Figures S1–S5 and S7.

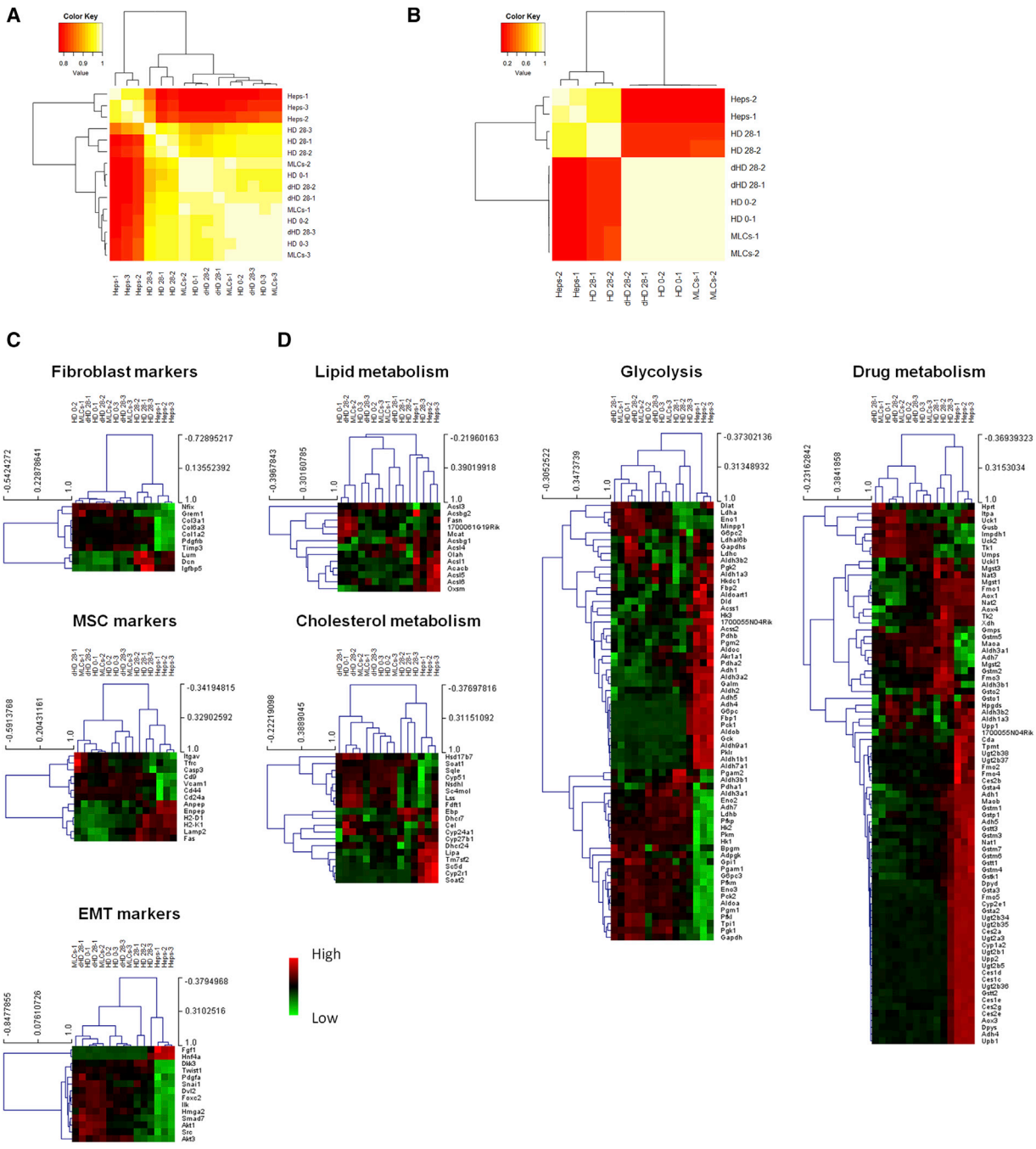

(legend on next page)

both general (e.g., cell cycle) and specific functions (e.g., lysosome and metabolism) were demonstrated (Table S1). A substantial overlap of KEGG pathways between HD and dHD was also observed. Moreover, microarray results revealed that upregulated pathways during HD substantially overlapped with downregulated pathways during dHD (Figure 2E, left panel), and vice versa (Figure 2E, right panel). These patterns indicated that dHD involved the pathways associated with HD and is essentially a reversal of the latter process.

ddHeps Exhibit Potential for Multi-lineage Differentiation

To investigate whether ddHeps regained multi-lineage differentiation potential, an essential function of MSCs, we examined their hepatogenic, osteogenic, and adipogenic differentiation capabilities. Hepatic induction caused ddHeps to become functional dHeps, evidenced by morphological changes, the capacity for glycogen storage and albumin production (Figure 3A), as well as the re-expression of hepatogenic-specific genes. Positive function assays, including glycogen storage, albumin production, and generation of urea, and downregulation of Ki67 also supported the manifestation of hepatic re-differentiation (Figures 3B and 3C). Next, osteogenic differentiation of ddHeps was evidenced by morphologic change, alkaline phosphatase activity, and calcium mineralization of the extracellular matrix (Figure 3D), visible through von Kossa and alizarin red S staining. Osteogenic-specific gene expression was also increased significantly (Figure 3E). Finally, ddHeps differentiation into adipocytes was shown by the accumulation of neutral lipid vacuoles (Figure 3F), positive oil red O staining, and increased adipogenic-specific gene expression (Figure 3G).

To further confirm dHD and to rule out the possibility of incomplete HD, we sorted dHeps by staining for CD26, which is only expressed on mature hepatocytes but not in MSCs or immature hepatic progenitor cells. After dHD for 4 weeks, ddHeps derived from $CD26^{high}$ dHeps expressed a typical MSC phenotype (Figures S3A–S3D) and regained multi-lineage differentiation potentials (Figures S3E–S3G). Expression of lineage-specific genes in ddHeps upon various lineage induction is similar to that of primary MSCs (Figures S3E–S3G). ddHeps lacked cell-surface antigens CD45 and CD90 (Figure S3D) and did not express markers of liver progenitors reported in the literature (Chen et al., 2012; Oikawa et al., 2009). Thus, ddHeps are indeed closer to MSCs rather than committed liver progenitor cells, oval cells, or hepatoblasts.

Hepatic Lineage Reversibility Is Associated with MET and EMT

Mesenchymal-to-epithelial transition (MET) and epithelial-to-mesenchymal transition (EMT) are reversible processes that dictate cell morphology, migration, and differentiation (Thiery and Sleeman, 2006). To examine whether MET and EMT were involved during HD and dHD, we surveyed the expression of mesenchymal and epithelial marker genes. During HD of MSCs, epithelial markers such as *Cdh1*, *Epcam*, *Gja1*, and *Tjp1* were upregulated, whereas mesenchymal markers such as *Vim*, *Fn1*, *Acta1*, and *Acta2*, as well as the master EMT regulators *Tgfb1* and *Snai1*, were downregulated. A reverse pattern was observed during dHD (Figures S4A–S4C). In addition, migratory capacity was decreased after HD and recovered upon dHD (Figure S4D). We concluded that HD is associated with MET, whereas dHD is associated with EMT.

Reversible HD Also Occurs in Human MSCs

We applied the same approach to induce HD and dHD in human MSCs. Reversible changes of morphology, hepatogenic-specific gene profile, hepatic functions, MET markers, and migration capacity (Figures S5A–S5F) were also observed in human MSCs. Moreover, human ddHeps retained multi-lineage differentiation potential (Figures S5G–S5I). Overall, the results from mouse and human MSCs were consistent; the fate of human MSCs could also be reversed after differentiation into the hepatic lineage.

DNA Methyltransferases Regulate HD of MSCs and dHD

To investigate the role of epigenetic effects during HD and dHD of MSCs, we used real-time qRT-PCR to screen the expression of 19 epigenetic modulators in DNA and histone methylation pathways (Figure 4A). We found that

Figure 2. Microarrays and High-Density Antibody Arrays of Transcriptomes and Proteomes Reveals Hepatogenic Differentiation and De-differentiation

(A–D) Hierarchical clustering via correlations in the transcriptome (A) and the proteome (B). Expression patterns of genes involved in fibroblast, MSC, and EMT markers (C). Expression patterns of genes involved in lipid, glucose, cholesterol, and drug metabolism (D). Each column represents a single array sample.

(E) Venn diagrams showing the overlap of up- and downregulated KEGG pathways within the transcriptome during HD and dHD. "HD 0" refers to MSCs; "HD 28" refers to MSC-derived dHeps after 28 days of HD; "dHD 28" refers to dHep-derived ddHeps after 28 days of dHD; "Heps" refers to mouse primary hepatocytes; "MLCs" refers to MSC-like cells derived from Heps.

See also Tables S1 and S2.

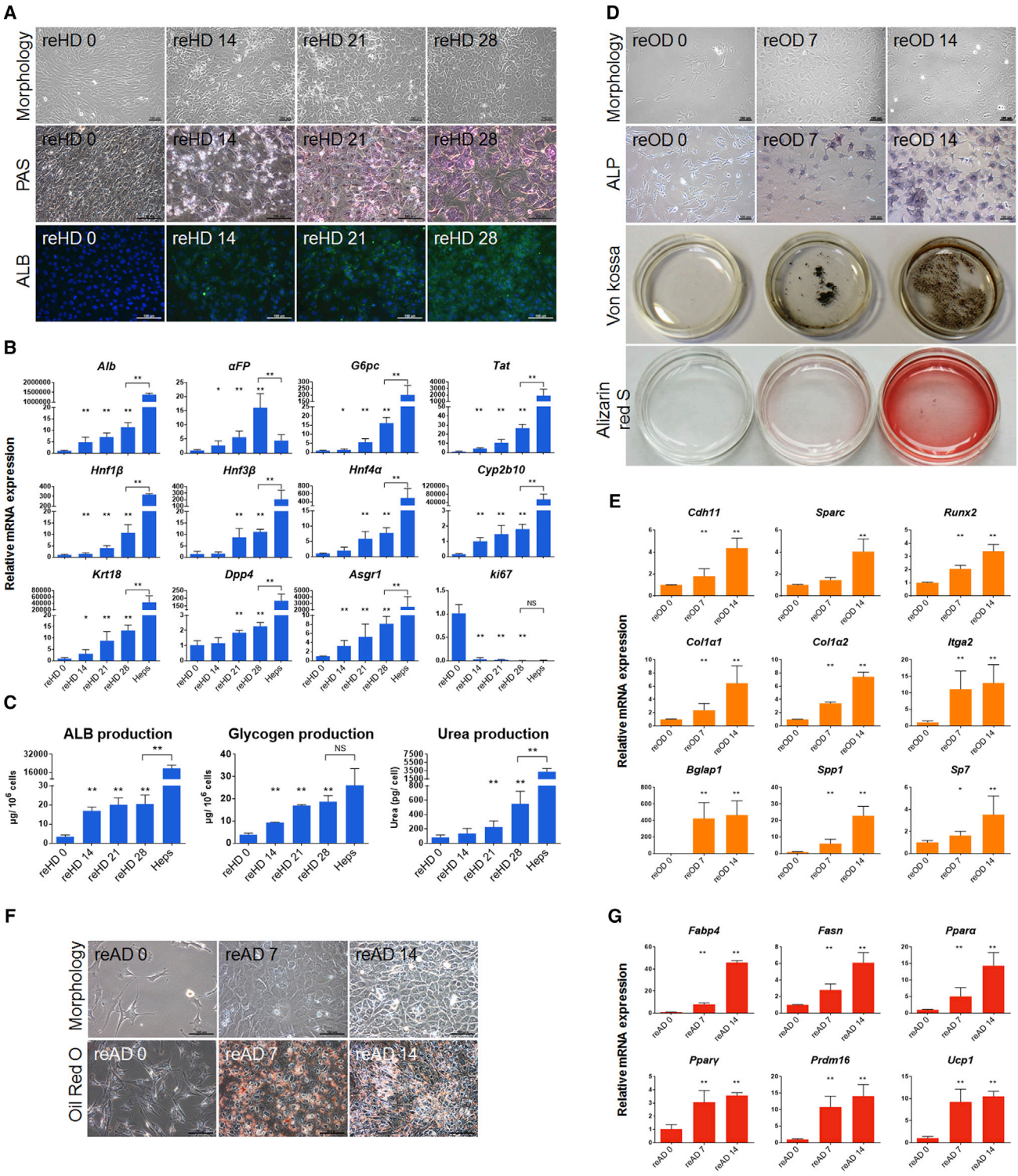

Figure 3. dHeps Can Also De-differentiate and Regain Multi-lineage Differentiation Potentials

(A) Representative morphological changes and staining (PAS and albumin [ALB]) of ddHeps during hepatogenic re-differentiation (reHD).

(B) qRT-PCR of hepatogenic-specific genes inddHep-derived dHeps (n = 3 independent experiments).

(C) Hepatic functions of ddHep-derived dHeps were evaluated with albumin production (n = 3 independent experiments), glycogen storage (n = 6 independent experiments), and urea production (n = 3 independent experiments).

(legend continued on next page)

DNMT1 expression was decreased during HD but was strongly increased after dHD (Figures 4A and 4B), to levels higher than the nascent MSCs (HD 0). In contrast, DNMT3a and DNMT3b expression was increased during HD and returned to the original levels similar to MSCs after dHD. In addition, pretreatment with 5-azacytidine (a pan-DNMT inhibitor) reduced global DNA methylation in MSCs (Figure 4C). Over time, increasing doses of 5-azacytidine enhanced hepatogenic-specific gene expression and hepatic functions (Figures 4D and 4E). These results indicated that DNMTs are involved in the HD of MSCs.

We then performed loss-of-function assays to determine the roles of individual DNMTs in HD. Small interfering RNAs (siRNAs) against DNMT1, DNMT3a, and DNMT3b were added individually during HD (Figures 4F and 4G). The results revealed that in HD 14, DNMT1 knockdown significantly enhanced the expression of hepatogenic-specific genes, MET/EMT markers (Figure 4H), and the metabolically important cytochrome P450 (CYP) family members (Figure 4I). Furthermore, hepatic functions were enhanced (Figure 4J). An acceleration of HD via DNMT1 knockdown was observed: HD 14 cells with DNMT1 knockdown are similar to HD 28 cells in terms of gene expression and hepatic functions (Figures 4H–4J). Knockdown of DNMT3a only downregulated several hepatogenic markers (Figure 4H), but significantly reduced the expression of all CYP enzymes examined (Figure 4I). Knockdown of DNMT3b had no influence on HD (Figures 4H–4J). Simultaneous silencing of DNMT3a and DNMT3b did not further repress HD at day 14 (Figures 4H–4J). In terms of morphological changes during dHD, DNMT1 knockdown maintained epithelial morphology and increased albumin expression compared with parental and control groups. In contrast, DNMT3a knockdown promoted a fibroblast-like morphology and decreased albumin expression (Figures 4K and 4L). Collectively, these data showed that DNMT1 extensively regulated hepatic lineage commitment but DNMT3a specifically regulated the CYP family during the HD of MSCs. Moreover, DNMT1 silencing accelerated HD.

Identification of Signaling Pathways Involved in DNMT-Modulated HD and dHD

To identify the signaling pathways involved in DNMT-dependent HD, we integrated the microarray and protein array data associated with DNMT1 expression. Among 15 candidate genes, four (*Tgfb1*, *Thbs1*, *Thbs2*, and *Thbs3*) were involved in the TGFβ signaling pathways. Among these four, *Tgfb1* was highly expressed in both arrays (Figure 5A). Increased TGFβ1 expression was strongly associated with reversible differentiation (Figures 5B and S5E).

To test how DNMTs responded to TGFβ1, we altered the concentrations of TGFβ1 during HD. As TGFβ1 dosage increased, DNMT1 expression also increased in dHeps, whereas DNMT3a and DNMT3b expression decreased (Figure 5C). These effects were eliminated by LY-364947, an Alk-5 (TGFβRI/II) inhibitor, indicating that extracellular TGFβ1 signaling is Alk-5 dependent. To identify the signaling pathways involved in TGFβ1-regulated DNMT expression during HD, we tested both Smad and non-Smad signaling pathway inhibitors (Figure 5D). We showed that PD0325901 and SIS3 treatment reversed DNMT1 upregulation, SB203580 and LY294002 treatment reversed DNMT3a/3b downregulation, and SP600125 treatment did both. Therefore, TGFβ1 may regulate DNMT1 and DNMT3a/3b together via the JNK pathway, whereas it separately regulates DNMT1 via the ERK1/2 and canonical Smad2/3 pathways, as well as DNMT3a/3b via the p38 and PI3K-Akt pathways. Of note, neither DNMT knockdowns (Figures 5E and 5F) nor 5-azacytidine pretreatment (Figure 5G) affected TGFβ1 expression. These results demonstrated that DNMTs regulate HD in response to TGFβ1 signaling. Moreover, a feedback loop does not appear to exist in the TGFβ1-DNMT axis during the HD of MSCs.

To determine whether the downregulation of TGFβ1 signaling is essential for HD, we treated MSCs with TGFβ1 during HD. Our results showed that TGFβ1 repressed morphologic changes (Figure 5H), hepatogenic-specific gene expression (Figure 5I), and hepatic functions (Figure 5J), whereas it increased cell migratory capacity (Figure 5K). All effects from TGFβ1 treatment were reduced or eliminated by LY-364947. Our results confirmed that TGFβ1 signaling must be downregulated for the HD of MSCs.

Murine Hepatocytes Can Be Converted to Functional MSC-like Cells

Since dHeps are similar to hepatic progenitors and are different from Heps, we further investigate whether similar phenomenon of de-differentiation from dHeps to MSCs can

(D) Representative morphological changes and staining (alkaline phosphatase [ALP], von Kossa, and alizarin red S) of ddHeps during osteogenic re-differentiation (reOD).

(E) qRT-PCR of osteogenic-specific genes in ddHep-derived osteoblasts (n = 3 independent experiments).

(F) Representative morphological changes and staining (oil red O) of ddHeps during adipogenic re-differentiation (reAD).

(G) qRT-PCR of adipogenic-specific genes in ddHep-derived adipocytes (n = 3 independent experiments).

All quantitative data are presented as means ± SD. Statistical analyses were performed using Student's paired t test, with significance set at *p < 0.05, **p < 0.005. NS, not significant. Scale bars represent 100 μm for phase contrast and staining. See also Figures S5 and S7.

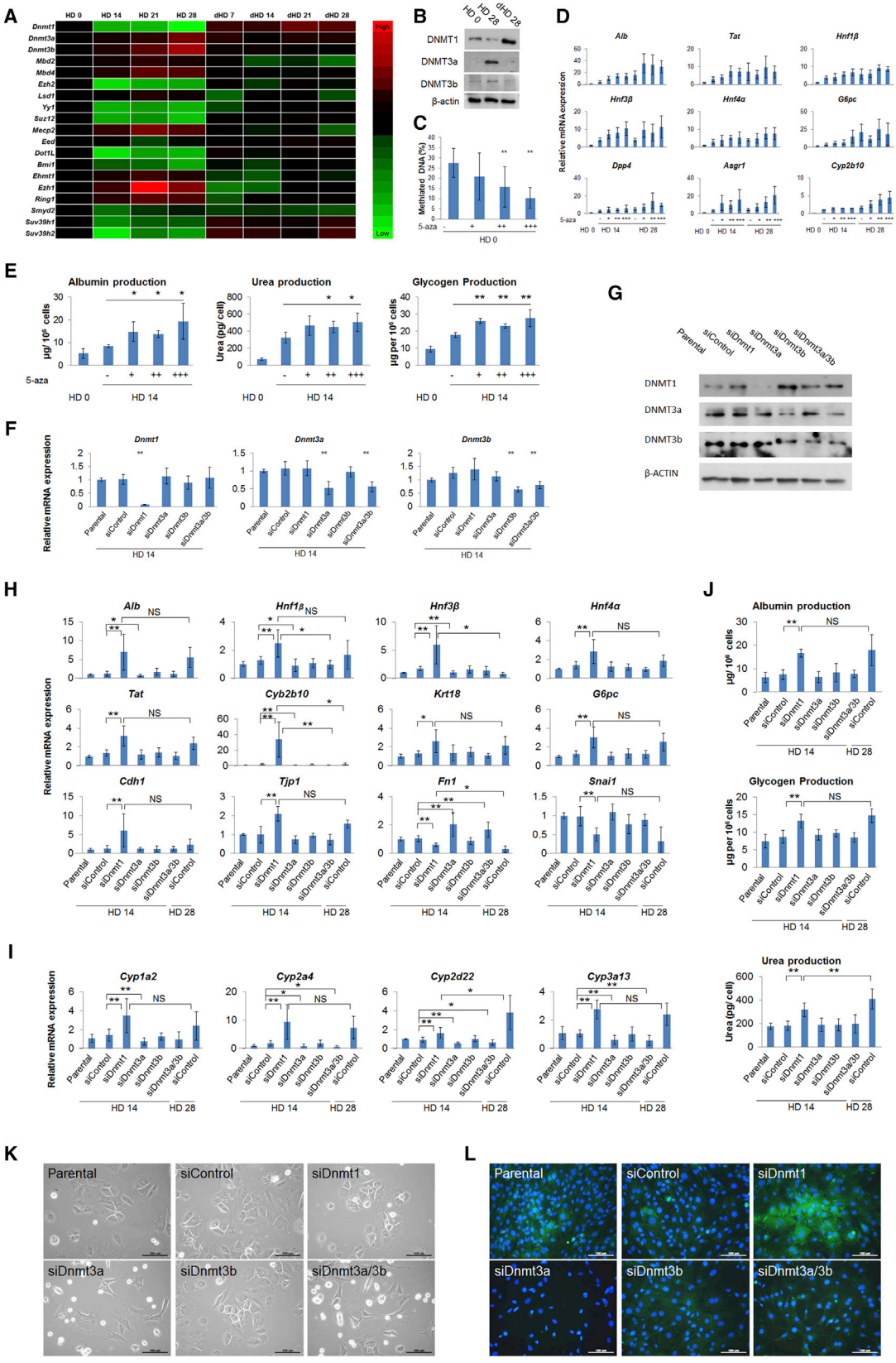

(legend on next page)

also occur in Heps. To investigate whether TGFβ1 can induce lineage conversion in hepatocytes, we treated primary hepatocytes with TGFβ1 or TGFβ1 receptor inhibitor (LY-364947) for 3–7 days. Treatment of Heps with TGFβ1 for 7 days resulted in a fibroblast-like morphology and a loss of hepatogenic-specific genes. These effects were eliminated by LY-364947 administration (Figure S7). Expression of hepatogenic-specific genes was increased in LY-364947-treated Heps compared with medium-only control on day 7 (Figure S7). Blocking of the endogenous TGFβ1 signaling repressed the loss of hepatocyte characteristics, supporting that TGFβ1 is necessary and sufficient to trigger hepatic-mesenchymal lineage conversion. Currently known actions of TGFβ1 include inducing apoptosis, de-differentiating fetal hepatocytes to liver progenitors, and mediating the acquisition of mesenchymal morphology (Caja et al., 2011; Tu et al., 2014). Additionally TGFβ1 is involved in the myofibroblastic (Kakudo et al., 2012), chondrogenic (Toh et al., 2005), and cardiomyogenic differentiation (Mohanty et al., 2013) of MSCs. Therefore, we attempted to convert purified $CD26^{high}$ Heps to MSC-like cells (MLCs) by treating them with stepwise reduction of TGFβ1 (Figure 6A). This stepwise protocol converted $CD26^{high}$ Heps to an MSC-like status in terms of morphology, hepatogenic-specific gene expression, cell-surface phenotype, hepatic functions (Figures 6B–6G), and EMT markers (Figures 6H and 6I). MLCs re-entered into cell cycle and increased the cell number in culture, and re-thawed MLCs retained proliferative capacity (Figures 6J and 6K).

The transcriptomes and proteomes of MLCs and MSCs were similar (Figures 2A and 2B). The two cell types also exhibited similarities in the expression of metabolism-related genes (Figure 2D) and other gene sets (Figure 2C). Gene ontology analyses revealed substantial overlap of enriched pathways during Hep lineage conversion to MLCs and during reversible HD of MSCs (Figure 2E and Table S2). After treatment with TGFβ1 we noted the induction of endogenous TGFβ1 expression in MLCs, which was maintained after exogenous TGFβ1 removal (Figures 6H and 6L). In addition, DNMT1 knockdown prevented TGFβ1-induced loss of hepatogenic-specific genes in Heps (Figure 6M), and DNMT expression patterns were consistent between Hep-derived MLCs and MSCs (Figures 6N and 6O), providing evidence that DNMTs mediated the TGFβ1-induced lineage conversion of Heps. Finally, MLCs possessed multi-lineage potentials comparable with those of MSCs (Figures 7A–7G); while they exhibited higher hepatic potential, particularly in the expression of CYP family enzymes (Figure 7B). Together, these results indicated that Hep-converted MLCs are very similar to primary MSCs.

Reversible Differentiation Does Not Induce Tumorigenicity

Long-term culture expansion, changes to methylation states, and DNMT deficiency may cause genomic instability and lead to malignant transformation (Foudah et al., 2009; Josse et al., 2010; Karpf and Matsui, 2005; Miura et al., 2006; Rosland et al., 2009). Moreover, DNMT1 expression has been associated with hepatocellular carcinomas (Raggi et al., 2014). We found a deletion of Y chromosome and a duplication of chromosome 16 after the long-term differentiation and de-differentiation process revealed by comparative genomic hybridization arrays (n = 1, data not shown). To test whether differentiation and de-differentiation process induces tumorigenicity, we subcutaneously inoculated nude mice with mouse MSCs, ddHeps, dHeps with siRNA against DNMT1, and MLCs. We observed no tumor formation after 13 weeks, indicating that tumorigenicity is not induced by long-term reversible differentiation, genetic manipulation of DNMTs, or lineage conversion (Figures 7H and 7I).

Figure 4. DNA Methyltransferases Regulate Hepatogenic Differentiation and De-differentiation of Mouse MSCs

(A) A heatmap summarizing relative mRNA levels of 19 epigenetic modulators (n = 4).

(B) Representative immunoblot for DNA methyltransferases (DNMTs) expression in MSCs during HD and dHD.

(C–I) DNMT-inhibitor (5-azacytidine [5-aza]) treatment inhibited global DNA methylation (n = 3 independent experiments). After 14 days of HD, enhancement from pan-DNMT inhibitor pretreatment occurred in hepatogenic-specific gene expression, as visualized with qRT-PCR (n = 4 independent experiments) (D), and in hepatic functions (E), as represented by albumin production (n = 2 independent experiments, four technical replicates), glycogen storage (n = 2 independent experiments, 12 technical replicates), and urea production (n = 2 independent experiments, five technical replicates). Symbols indicate treatments with different 5-aza concentrations (+, 0.5 μM; ++, 1 μM; +++, 2 μM). Efficiency of DNMT knockdown determined with qRT-PCR (F) (n = 6 independent experiments) and immunoblot (G) at HD 14. Knockdown of DNMTs altered hepatogenic-specific genes, EMT/MET markers (H), and CYP enzymes (I) at HD 14 (n = 6 independent experiments).

(J–L) Knockdown of DNMTs altered hepatic functions at HD 14, as represented by albumin production (n = 6 independent experiments), glycogen storage (n = 6 independent experiments), and urea production (n = 6 independent experiments). Knockdown of DNMTs altered cellular morphology at dHD 3 (K) and modulated albumin expression, as seen in the representative images of immunocytochemical staining (L).

All quantitative data are presented as means ± SD. Statistical analyses were performed using Student's paired t test, with significance set at *p < 0.05, **p < 0.005. NS, not significant. Scale bars represent 100 μm for phase contrast and staining. See also Figure S7.

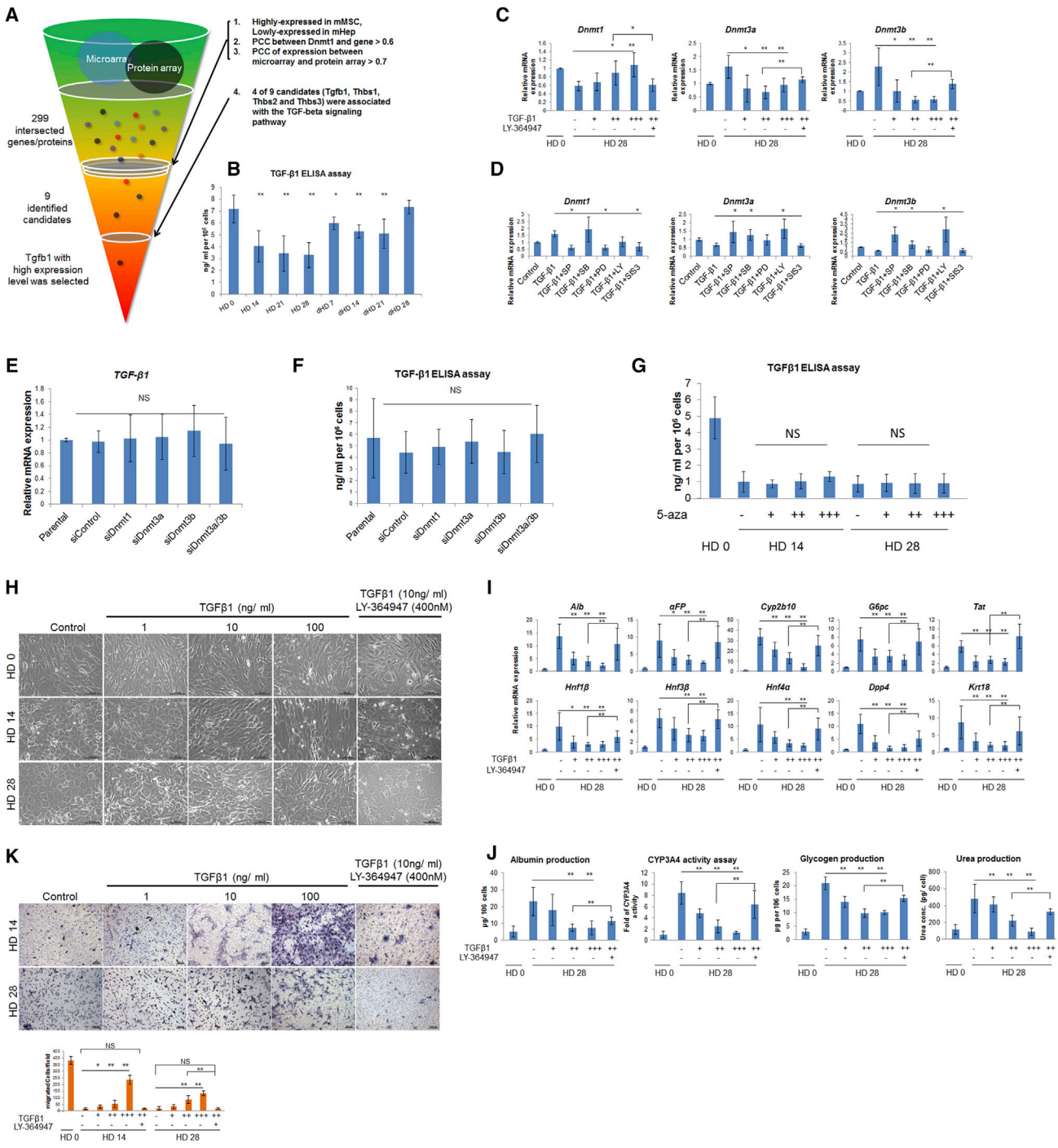

Figure 5. TGFβ1 Regulates DNMTs and Represses Hepatogenic Differentiation of Mouse MSCs

(A) Schematic illustration of signaling pathways. PCC, Pearson's correlation coefficient.

(B) ELISA results for TGFβ1 expression of MSCs during HD and dHD (n = 5 independent experiments).

(C) qRT-PCR of DNMTs from MSCs treated with TGFβ1 during HD (n = 6 independent experiments). Symbols indicate treatments of different TGFβ1 concentrations (+, 1 ng/mL; ++, 10 ng/mL; +++, 100 ng/mL).

(D–F) qRT-PCR of DNMTs from MSCs treated with TGFβ1 and various inhibitors during HD (n = 4 independent experiments) (D). LY-364947, Alk-5 inhibitor, 400 nM; SIS3, Smad2/3 inhibitor, 10 μM; SP600125, JNK inhibitor, 30 μM; SB203580, p38 inhibitor, 30 μM; PD0325901, MEK-ERK1/2 inhibitor, 1 μM; and LY294002, PI3K-Akt inhibitor, 25 μM. The mRNA expression from each treatment was statistically

(legend continued on next page)

DISCUSSION

In this study, we show that hepatic lineages are reversible between adult MSCs and hepatocytes. Such reversibility is regulated by the TGFβ1-DNMT axis. To the best of our knowledge, this is also the demonstration that hepatocytes can be converted into multi-potent MLCs without ectopic gene delivery. Our findings support the occurrence of lineage reversibility in mammalian cells, indicating that such a phenomenon is not restricted to plants and non-mammalian vertebrates (Brockes, 1997; Brockes and Kumar, 2002; Weigel and Jurgens, 2002).

Our findings demonstrate a role of DNMTs in hepatic lineage reversibility of MSCs, with individual DNMTs exerting opposite effects; DNMT1 repressed HD and promoted dHD; while DNMT3a promoted HD and repressed dHD. The two enzymes seem to have both unique and overlapping target cytosine-phosphate-guanine (CpG) sites, as shown by the promotion of all hepatogenic-specific genes and hepatic functions via DNMT1 silencing, but a more specific repression of the CYP family via DNMT3a silencing (Figure 4). In addition, the inhibitory effect of DNMT1 appears to be more predominant than the activating effect of DNMT3a, because a pan-DNMT inhibitor resulted in the promotion of HD (Figure 4). Although DNMT3b expression is also strongly associated with HD and responded to TGFβ1 stimulation, DNMT3b knockdown fails to affect hepatic gene expression and function. While more data are necessary to clarify the function of DNMT3b in HD, we speculate that the enzyme may cooperate with other chromatin modifiers. Epigenetic effects exerted by these modifiers may have been sufficient for HD regulation, explaining why we do not observe significant changes resulting from DNMT3b knockdown (Baubec et al., 2015; Morselli et al., 2015).

In addition to demonstrating the importance of DNMTs, we show that TGFβ1 differentially regulated DNMTs, and that TGFβ1 is both necessary and sufficient to induce lineage conversion of hepatocytes into MLCs with phenotypes and multipotency resembling MSCs. Upon withdrawal of TGFβ1 on day 28, we observed that Hep-converted MLCs possessed MSC-like DNMTs expression patterns (Figures 6N and 6O) due to the induction of endogenous TGFβ1 expression (Figures 6H and 6L). This outcome supports the existence of an MSC-specific methylome that maintains MLC phenotypes and multipotency.

α-Fetoprotein (AFP) is a marker indicating early hepatic fate. Although AFP is not detectable in hepatocytes in vivo, expression of AFP may be detected in the in vitro culture conditions owing to a loss of contact (Gleiberman et al., 1989). Moreover, TGFβ1 downregulated albumin and AFP expression and induced fibroblast morphology and mesenchymal marker expression (mesenchymal fate) in Hep3B cells (Caja et al., 2011). Therefore, AFP may serve as a marker to distinguish hepatic fate from mesenchymal fate and allows us to track cellular conversion from the former to the latter.

Fibrosis is often a consequence of various chronic liver diseases and leads to hepatic failure as well as cancer. TGFβ1, a master inducer of EMT, orchestrates fibrogenesis. Persistent TGFβ1 stimulation converts both hepatocytes and MSCs into myofibroblasts and participates in liver fibrosis, and even contributes to the development of tumor (Sekiya et al., 2016). While blocking TGFβ signaling in hepatocytes alone attenuates liver fibrosis (Dooley et al., 2008) and facilitates liver regeneration (Karkampouna et al., 2016), MLCs may be at an intermediate state during the transition to myofibroblasts. Therefore, inhibition of the TGFβ1-DNMT axis in vivo may convert Hep-derived myofibroblasts back into MLCs or hepatocytes, and may attenuate liver fibrosis and facilitate liver regeneration. Our previous studies established a protocol for functional dHeps with therapeutic potentials when transplanted in vivo (Jiang et al., 2014; Kuo et al., 2008; Lee et al., 2004). However, dHeps required 28 days of in vitro differentiation, a lengthy duration that hampers their clinical application. In this study, we successfully accelerate differentiation to 14 days by silencing DNMT1 (Figure 4). Transplantation of dHeps with TGFβ receptor inhibitor or DNMT1 antagonist may stabilize hepatic characteristics of transplanted dHeps. On the other hand, although transplanted dHeps may de-differentiate

compared with a TGFβ1-treated group. Control refers to MSC-derived dHeps after 14 days. Results from qRT-PCR (E) (n = 6 independent experiments) and ELISA (F) (n = 3 independent experiments) of TGFβ1 expression at HD 14 after DNMT knockdown.

(G) DNMT-inhibitor pretreatment did not affect TGFβ1 expression (n = 3 independent experiments). Symbols indicate treatments with different 5-azacytidine concentrations (+, 0.5 μM; ++, 1 μM; +++, 2 μM).

(H) Representative morphological changes of MSCs treated with TGFβ1 during HD.

(I) qRT-PCR of hepatogenic-specific genes in dHeps under TGFβ1 treatment (n = 5 independent experiments).

(J) Hepatic functions of dHeps under TGFβ1 treatment, as represented by albumin production (n = 7 independent experiments), glycogen storage (n = 5 independent experiments), and urea production (n = 6 independent experiments).

(K) Quantification of transwell migration assay (n = 3 independent experiments) of MSCs treated with TGFβ1 during HD.

All quantitative data are presented as means ± SD. Statistical analyses were performed using Student's paired t test, with significance set at *p < 0.05, **p < 0.005. NS, not significant. Scale bars represent 100 μm for phase contrast and staining. See also Figures S6 and S7.

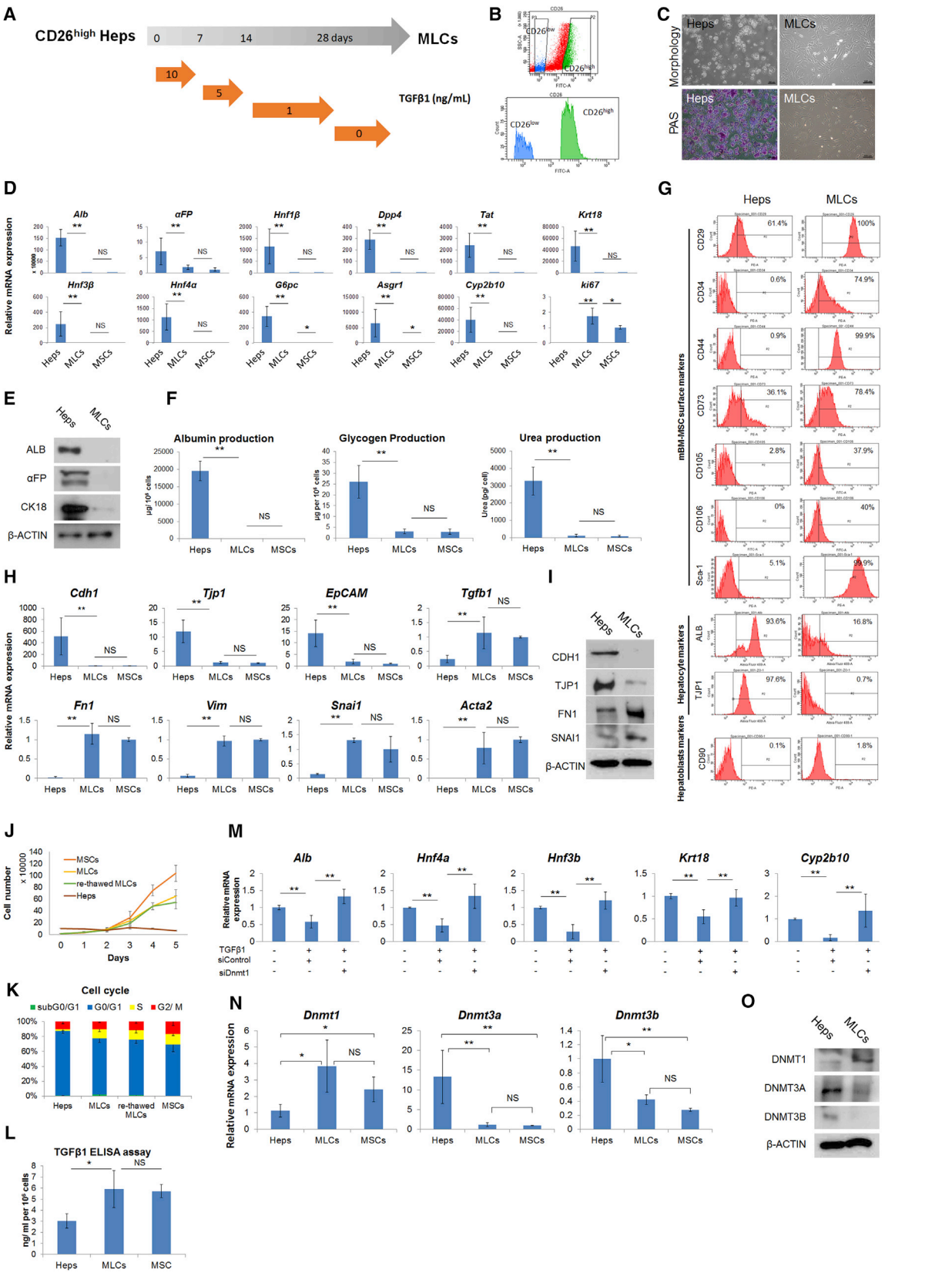

(legend on next page)

into ddHeps, ddHeps may promote liver regeneration like MSCs through immunomodulation and trophic support (Christ et al., 2015). Hep-converted MLCs have proliferation ability and higher hepatic lineage potential (Figure 7B). Therefore, these cells may also serve as an alternative cell source for liver regeneration (Du et al., 2014; Takeuchi et al., 2015).

In summary, hepatic lineage reversibility exists and is regulated by the previously unrecognized TGFβ1-DNMT axis. The ability to convert Heps into MLCs with altered extracellular concentrations of TGFβ1 suggests that terminally differentiated hepatocytes may exhibit considerably greater plasticity than previously believed. Our findings have not only offered therapeutic insights for use of MSCs or differentiated hepatic progenies for transplantation to treat liver diseases, but have also contributed to the development of approaches for achieving tissue regeneration through promoting de-differentiation and lineage conversion in vivo.

EXPERIMENTAL PROCEDURES

All animal studies were approved by the Taipei Veterans General Hospital Institutional Animal Care and Use Committee (IACUC 2014-043).

Cell Culture and Reagents

MSCs were obtained from bone marrow and were maintained in culture as previously described (Jiang et al., 2014; Lee et al., 2004). The characteristics of MSCs were confirmed by their expression of surface markers and ability of multi-potent differentiation into osteoblasts, adipocytes, and chondroblasts in vitro (Figure S1). Mouse MSCs (mMSCs) were cultured in an mMSC-maintenance medium, consisting of low-glucose DMEM supplemented with 10% fetal bovine serum (FBS) (Gibco, Thermo Fisher Scientific); human MSCs (hMSCs) were cultured in hMSC-maintenance medium, consisting of Iscove's modified Dulbecco's medium (IMDM) supplemented with 10% FBS, 10 ng/mL epidermal growth factor, and 10 ng/mL basic fibroblast growth factor (bFGF) (R&D Systems). Human primary hepatocytes (hHeps) were purchased from ScienCell and cultured in Hepatocyte Medium (ScienCell). Mouse hepatocytes were isolated from 10- to 12-week-old BALB/c mice with a protocol in the literature (Klaunig et al., 1981a, 1981b), and were cultured in Hep-maintenance medium consisting of DMEM/F12 supplemented with 10% FBS. FL83B cells were cultured in F-12K medium (Gibco, Thermo Fisher Scientific) supplemented with 10% FBS. Low-glucose DMEM, IMDM, DMEM/F12, 5-azacytidine, TGFβ1, and LY-364947 were purchased from Sigma-Aldrich; SP600125, SB203580, PD325901, LY294002, and SIS3 were purchased from Abcam.

Hepatogenic Differentiation and De-differentiation

HD was induced following our previously reported two-step protocol (Lee et al., 2004). In brief, $1.0 \times 10^4/cm^2$ MSCs were seeded and cultured for 2 days in the maintenance medium. Two days post seeding, cells were treated with a step-1 differentiation medium, consisting of IMDM supplemented with 20 ng/mL hepatocyte growth factor and 10 ng/mL bFGF (R&D Systems), and 0.61 g/L nicotinamide (Sigma-Aldrich). Seven days later, cells were treated with a step-2 differentiation medium, consisting of IMDM supplemented with 20 ng/mL oncostatin M (Invitrogen), 1 μmol/L dexamethasone (Sigma-Aldrich), and 50 mg/mL ITS+ premix (BD Biosciences) for 3 weeks. The differentiation medium was changed

Figure 6. Stepwise TGFβ1 Treatment Converts Mouse Primary Hepatocytes into MSC-like Cells though Initiating the Secretion of Endogenous TGFβ1

(A) Schematic illustration of the experimental approach.

(B) Representative flow-cytometry plots showing CD26 expression and the gating strategies used to isolate $CD26^{low}$ and $CD26^{high}$ hepatocytes.

(C) Representative morphology and PAS staining for MLCs.

(D and E) Loss of hepatogenic-specific gene expression in MLCs, analyzed with qRT-PCR (D) (n = 4 independent experiments) and immunoblot (E).

(F) Loss of hepatic function in MLCs, as represented by albumin production (n = 4 independent experiments), glycogen storage (n = 3 independent experiments), and urea production (n = 4 independent experiments).

(G) Surface phenotypic characterization analyzed with flow cytometry.

(H and I) Gene expression of MET/EMT markers during de-differentiation of mouse Heps, analyzed with qRT-PCR (H) (n = 4 independent experiments) and immunoblot (I).

(J and K) Cell numbers counted at each time point (n = 3 independent experiments) (J) and relative percentage of cells in various cell-cycle phases (n = 5 independent experiments) (K). "Re-thawed MLCs" refers to MLCs re-thawed from cryopreservation and cultured for another week at least.

(L) ELISA of TGFβ1 expression in Heps, MLCs, and MSCs (n = 4 independent experiments); the amount of TGFβ1 from serum has been deducted.

(M) qRT-PCR of hepatogenic-specific genes in mouse Heps under TGFβ1 and siDnmt1 treatment for 3 days (n = 3 independent experiments). The plus and minus symbols respectively indicate treatments with and without TGFβ1 (10 ng/mL), siControl (50 nM), and siDnmt1 (50 nM).

(N and O) Expression of DNMTs in hepatocytes, MLCs, and MSCs, analyzed by qRT-PCR (N) (n = 4 independent experiments) and immunoblot (O).

*$p < 0.05$, **$p < 0.005$. NS, not significant. Scale bars represent 100 μm for phase contrast and staining. See also Figures S6 and S7.

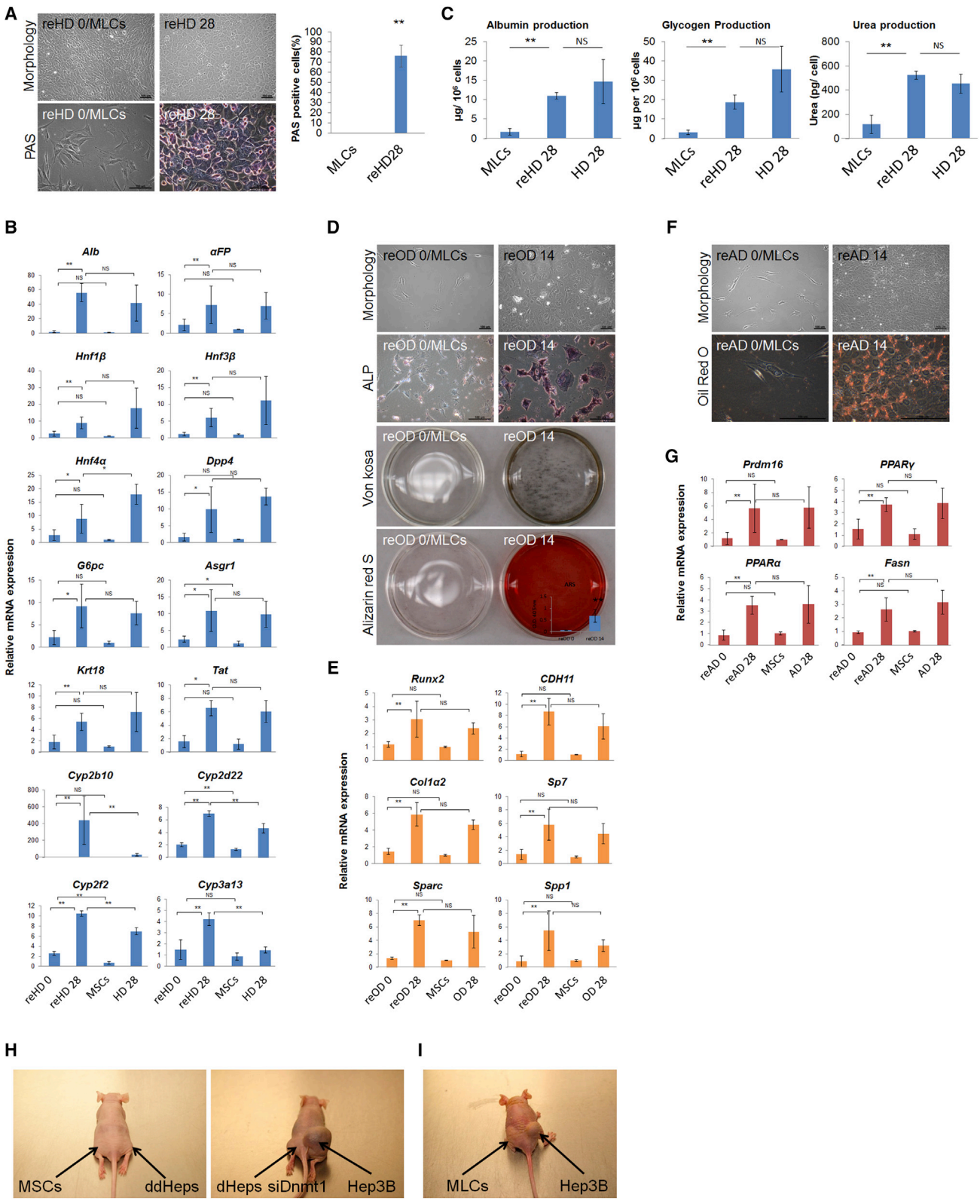

(legend on next page)

once per week. To induce dHD in MSC-derived dHeps, we replaced the step-2 medium with maintenance medium (low-glucose DMEM supplemented with 10% FBS). A protocol with stepwise reduction of TGFβ1 was used to induce the lineage conversion of Heps. Specifically, Heps were cultured in an mMSC-maintenance medium with 10 ng/mL TGFβ1 for the first 7 days, then with 5 ng/mL TGFβ1 for another 7 days, and finally with 1 ng/mL TGFβ1 for the following 14 days. After 28 days, cells were cultured in maintenance medium without TGFβ1.

Other experimental procedures and statistical analysis are described in Supplemental Experimental Procedures.

ACCESSION NUMBERS

With regard to transcript profiling the accession numbers are: microarray, GEO: GSE73617; protein array, GEO: GSE73762.

SUPPLEMENTAL INFORMATION

Supplemental Information includes Supplemental Experimental Procedures, seven figures, and three tables and can be found with this article online at http://dx.doi.org/10.1016/j.stemcr.2017.05.008.

AUTHOR CONTRIBUTIONS

C.-W.L. designed the study, performed experiments, analyzed data, and wrote the manuscript; W.-C.H. and H.-D.H. performed microarray and protein array analysis; Y.-H.H., J.H.H., and M.-H.Y. provided feedback for the manuscript; V.W.Y. and O.K.L. edited the manuscript and supervised the study.

ACKNOWLEDGMENTS

This work was supported in part by the Novel Bioengineering and Technological Approaches to Solve Two Major Health Problems in Taiwan sponsored by the Taiwan Ministry of Science and Technology Academic Excellence Program under grant number MOST 105-2633-B-009-003. The authors acknowledge financial support from the Ministry of Science and Technology, Taiwan (MOST103-2314-B-010-053-MY3, MOST 106-2321-B-010-008, MOST 106-2911-I-010-502, and MOST 105-2633-B-010-002). This study was also supported by Aiming for the Top University Plan, a grant from Ministry of Education. The authors also acknowledge the technical support provided by Flow Cytometry Core Facility of National Yang Ming University and Imaging Core Facility of Nanotechnology of the UST-YMU. We acknowledge Prof. Ting-Fen Tsai from National Yang-Ming University, Taiwan for the kind gift of E12.5 fetal livers and thank Prof. Chi-Chang Juan from National Yang-Ming University, Taiwan for the kind gift of FL83B cells.

Received: June 13, 2016
Revised: May 4, 2017
Accepted: May 5, 2017
Published: June 8, 2017

REFERENCES

Baubec, T., Colombo, D.F., Wirbelauer, C., Schmidt, J., Burger, L., Krebs, A.R., Akalin, A., and Schubeler, D. (2015). Genomic profiling of DNA methyltransferases reveals a role for DNMT3B in genic methylation. Nature *520*, 243–247.

Brockes, J.P. (1997). Amphibian limb regeneration: rebuilding a complex structure. Science *276*, 81–87.

Brockes, J.P., and Kumar, A. (2002). Plasticity and reprogramming of differentiated cells in amphibian regeneration. Nat. Rev. Mol. Cell Biol. *3*, 566–574.

Caja, L., Bertran, E., Campbell, J., Fausto, N., and Fabregat, I. (2011). The transforming growth factor-beta (TGF-beta) mediates acquisition of a mesenchymal stem cell-like phenotype in human liver cells. J. Cell. Physiol. *226*, 1214–1223.

Chen, Y., Wong, P.P., Sjeklocha, L., Steer, C.J., and Sahin, M.B. (2012). Mature hepatocytes exhibit unexpected plasticity by direct dedifferentiation into liver progenitor cells in culture. Hepatology *55*, 563–574.

Christ, B., Bruckner, S., and Winkler, S. (2015). The therapeutic promise of mesenchymal stem cells for liver restoration. Trends Mol. Med. *21*, 673–686.

Dooley, S., Hamzavi, J., Ciuclan, L., Godoy, P., Ilkavets, I., Ehnert, S., Ueberham, E., Gebhardt, R., Kanzler, S., Geier, A., et al. (2008). Hepatocyte-specific Smad7 expression attenuates TGF-beta-mediated fibrogenesis and protects against liver damage. Gastroenterology *135*, 642–659.

Figure 7. Mouse Hepatocyte-Derived MSC-like Cells Retain Multi-lineage Differentiation Potential In Vitro

(A) Representative morphology and PAS staining for MLC-derived dHeps.
(B) qRT-PCR analysis of hepatogenic-specific gene expression (n = 3 independent experiments).
(C) Cellular hepatic functions (n = 4 independent experiments).
(D) Representative morphology and staining (alkaline phosphatase [ALP], von Kossa, and alizarin red S [n = 3 independent experiments]) of MLC-derived osteocytes.
(E) qRT-PCR analysis of osteogenic-specific gene expression (n = 3 independent experiments).
(F) Representative morphology and staining (oil red O) of MLC-derived adipocytes.
(G) qRT-PCR analysis of adipogenic-specific gene expression (n = 3 independent experiments).
(H) Representative photograph comparing tumorigenicity from mouse MSCs, ddHeps, dHeps with siDnmt1, and Hep3B cells in BALB/c nude mice after inoculation for 13 weeks (n = 6 mice per group). Black arrows indicate injection sites.
(I) Representative photograph comparing tumorigenicity of MLCs and Hep3B after inoculation for 8 weeks. Black arrows indicate injection sites.
All quantitative data are presented as means ± SD. Statistical analyses were performed using Student's paired t test, with significance set at *p < 0.05, **p < 0.005. NS, not significant. Scale bars represent 100 μm for phase contrast and staining.

Du, Y., Wang, J., Jia, J., Song, N., Xiang, C., Xu, J., Hou, Z., Su, X., Liu, B., Jiang, T., et al. (2014). Human hepatocytes with drug metabolic function induced from fibroblasts by lineage reprogramming. Cell Stem Cell *14*, 394–403.

Foudah, D., Redaelli, S., Donzelli, E., Bentivegna, A., Miloso, M., Dalpra, L., and Tredici, G. (2009). Monitoring the genomic stability of in vitro cultured rat bone-marrow-derived mesenchymal stem cells. Chromosome Res. *17*, 1025–1039.

Gailhouste, L., Gomez-Santos, L., Hagiwara, K., Hatada, I., Kitagawa, N., Kawaharada, K., Thirion, M., Kosaka, N., Takahashi, R.U., Shibata, T., et al. (2013). miR-148a plays a pivotal role in the liver by promoting the hepatospecific phenotype and suppressing the invasiveness of transformed cells. Hepatology *58*, 1153–1165.

Gleiberman, A.S., Sharovskaya, Y., and Chailakhjan, L.M. (1989). "Contact inhibition" of alpha-fetoprotein synthesis and junctional communication in adult mouse hepatocyte culture. Exp. Cell Res. *184*, 228–234.

Jiang, W.C., Cheng, Y.H., Yen, M.H., Chang, Y., Yang, V.W., and Lee, O.K. (2014). Cryo-chemical decellularization of the whole liver for mesenchymal stem cells-based functional hepatic tissue engineering. Biomaterials *35*, 3607–3617.

Jopling, C., Boue, S., and Izpisua Belmonte, J.C. (2011). Dedifferentiation, transdifferentiation and reprogramming: three routes to regeneration. Nat. Rev. Mol. Cell Biol. *12*, 79–89.

Josse, C., Schoemans, R., Niessen, N.A., Delgaudine, M., Hellin, A.C., Herens, C., Delvenne, P., and Bours, V. (2010). Systematic chromosomal aberrations found in murine bone marrow-derived mesenchymal stem cells. Stem Cells Dev. *19*, 1167–1173.

Kakudo, N., Kushida, S., Suzuki, K., Ogura, T., Notodihardjo, P.V., Hara, T., and Kusumoto, K. (2012). Effects of transforming growth factor-beta1 on cell motility, collagen gel contraction, myofibroblastic differentiation, and extracellular matrix expression of human adipose-derived stem cell. Hum. Cell *25*, 87–95.

Karkampouna, S., Goumans, M.J., Ten Dijke, P., Dooley, S., and Kruithof-de Julio, M. (2016). Inhibition of TGFbeta type I receptor activity facilitates liver regeneration upon acute CCl_4 intoxication in mice. Arch. Toxicol. *90*, 347–357.

Karpf, A.R., and Matsui, S. (2005). Genetic disruption of cytosine DNA methyltransferase enzymes induces chromosomal instability in human cancer cells. Cancer Res. *65*, 8635–8639.

Klaunig, J.E., Goldblatt, P.J., Hinton, D.E., Lipsky, M.M., Chacko, J., and Trump, B.F. (1981a). Mouse liver cell culture. I. Hepatocyte isolation. In Vitro *17*, 913–925.

Klaunig, J.E., Goldblatt, P.J., Hinton, D.E., Lipsky, M.M., and Trump, B.F. (1981b). Mouse liver cell culture. II. Primary culture. In Vitro *17*, 926–934.

Kuo, T.K., Hung, S.P., Chuang, C.H., Chen, C.T., Shih, Y.R., Fang, S.C., Yang, V.W., and Lee, O.K. (2008). Stem cell therapy for liver disease: parameters governing the success of using bone marrow mesenchymal stem cells. Gastroenterology *134*, 2111–2121, 2121.e1–3.

Lee, K.D., Kuo, T.K., Whang-Peng, J., Chung, Y.F., Lin, C.T., Chou, S.H., Chen, J.R., Chen, Y.P., and Lee, O.K. (2004). In vitro hepatic differentiation of human mesenchymal stem cells. Hepatology *40*, 1275–1284.

Li, E. (2002). Chromatin modification and epigenetic reprogramming in mammalian development. Nat. Rev. Genet. *3*, 662–673.

Makino, S., Fukuda, K., Miyoshi, S., Konishi, F., Kodama, H., Pan, J., Sano, M., Takahashi, T., Hori, S., Abe, H., et al. (1999). Cardiomyocytes can be generated from marrow stromal cells in vitro. J. Clin. Invest. *103*, 697–705.

Metcalf, D. (2007). Concise review: hematopoietic stem cells and tissue stem cells: current concepts and unanswered questions. Stem Cells *25*, 2390–2395.

Miura, M., Miura, Y., Padilla-Nash, H.M., Molinolo, A.A., Fu, B., Patel, V., Seo, B.M., Sonoyama, W., Zheng, J.J., Baker, C.C., et al. (2006). Accumulated chromosomal instability in murine bone marrow mesenchymal stem cells leads to malignant transformation. Stem Cells *24*, 1095–1103.

Miyajima, A., Tanaka, M., and Itoh, T. (2014). Stem/progenitor cells in liver development, homeostasis, regeneration, and reprogramming. Cell Stem Cell *14*, 561–574.

Mohanty, S., Bose, S., Jain, K.G., Bhargava, B., and Airan, B. (2013). TGFbeta1 contributes to cardiomyogenic-like differentiation of human bone marrow mesenchymal stem cells. Int. J. Cardiol. *163*, 93–99.

Morselli, M., Pastor, W.A., Montanini, B., Nee, K., Ferrari, R., Fu, K., Bonora, G., Rubbi, L., Clark, A.T., Ottonello, S., et al. (2015). In vivo targeting of de novo DNA methylation by histone modifications in yeast and mouse. Elife *4*, e06205.

Oikawa, T., Kamiya, A., Kakinuma, S., Zeniya, M., Nishinakamura, R., Tajiri, H., and Nakauchi, H. (2009). Sall4 regulates cell fate decision in fetal hepatic stem/progenitor cells. Gastroenterology *136*, 1000–1011.

Petersen, B.E., Grossbard, B., Hatch, H., Pi, L., Deng, J., and Scott, E.W. (2003). Mouse A6-positive hepatic oval cells also express several hematopoietic stem cell markers. Hepatology *37*, 632–640.

Pittenger, M.F., Mackay, A.M., Beck, S.C., Jaiswal, R.K., Douglas, R., Mosca, J.D., Moorman, M.A., Simonetti, D.W., Craig, S., and Marshak, D.R. (1999). Multilineage potential of adult human mesenchymal stem cells. Science *284*, 143–147.

Qiu, Q., Hernandez, J.C., Dean, A.M., Rao, P.H., and Darlington, G.J. (2011). CD24-positive cells from normal adult mouse liver are hepatocyte progenitor cells. Stem Cells Dev. *20*, 2177–2188.

Raggi, C., Factor, V.M., Seo, D., Holczbauer, A., Gillen, M.C., Marquardt, J.U., Andersen, J.B., Durkin, M., and Thorgeirsson, S.S. (2014). Epigenetic reprogramming modulates malignant properties of human liver cancer. Hepatology *59*, 2251–2262.

Rosland, G.V., Svendsen, A., Torsvik, A., Sobala, E., McCormack, E., Immervoll, H., Mysliwietz, J., Tonn, J.C., Goldbrunner, R., Lonning, P.E., et al. (2009). Long-term cultures of bone marrow-derived human mesenchymal stem cells frequently undergo spontaneous malignant transformation. Cancer Res. *69*, 5331–5339.

Sekiya, S., Miura, S., Matsuda-Ito, K., and Suzuki, A. (2016). Myofibroblasts derived from hepatic progenitor cells create the tumor microenvironment. Stem Cell Reports *7*, 1130–1139.

Snykers, S., Henkens, T., De Rop, E., Vinken, M., Fraczek, J., De Kock, J., De Prins, E., Geerts, A., Rogiers, V., and Vanhaecke, T.

(2009). Role of epigenetics in liver-specific gene transcription, hepatocyte differentiation and stem cell reprogrammation. J. Hepatol. *51*, 187–211.

Takeuchi, K., Goto, H., Ito, Y., Sato, M., Matsumoto, S., Senba, T., Yamada, H., and Umehara, K. (2015). Dehydroepiandrosterone sulfate and cytochrome P450 inducers alleviate fatty liver in male rats fed an orotic acid-supplemented diet. J. Toxicol. Sci. *40*, 181–191.

Tarlow, B.D., Pelz, C., Naugler, W.E., Wakefield, L., Wilson, E.M., Finegold, M.J., and Grompe, M. (2014). Bipotential adult liver progenitors are derived from chronically injured mature hepatocytes. Cell Stem Cell *15*, 605–618.

Thiery, J.P., and Sleeman, J.P. (2006). Complex networks orchestrate epithelial-mesenchymal transitions. Nat. Rev. Mol. Cell Biol. *7*, 131–142.

Toh, W.S., Liu, H., Heng, B.C., Rufaihah, A.J., Ye, C.P., and Cao, T. (2005). Combined effects of TGFbeta1 and BMP2 in serum-free chondrogenic differentiation of mesenchymal stem cells induced hyaline-like cartilage formation. Growth Factors *23*, 313–321.

Tsai, C.C., Su, P.F., Huang, Y.F., Yew, T.L., and Hung, S.C. (2012). Oct4 and Nanog directly regulate Dnmt1 to maintain self-renewal and undifferentiated state in mesenchymal stem cells. Mol. Cell *47*, 169–182.

Tu, X., Zhang, H., Zhang, J., Zhao, S., Zheng, X., Zhang, Z., Zhu, J., Chen, J., Dong, L., and Zang, Y. (2014). MicroRNA-101 suppresses liver fibrosis by targeting the TGFbeta signalling pathway. J. Pathol. *234*, 46–59.

Weigel, D., and Jurgens, G. (2002). Stem cells that make stems. Nature *415*, 751–754.

Wislet-Gendebien, S., Hans, G., Leprince, P., Rigo, J.M., Moonen, G., and Rogister, B. (2005). Plasticity of cultured mesenchymal stem cells: switch from nestin-positive to excitable neuron-like phenotype. Stem Cells *23*, 392–402.

Zhau, H.E., He, H., Wang, C.Y., Zayzafoon, M., Morrissey, C., Vessella, R.L., Marshall, F.F., Chung, L.W., and Wang, R. (2011). Human prostate cancer harbors the stem cell properties of bone marrow mesenchymal stem cells. Clin. Cancer Res. *17*, 2159–2169.